frontiers in Environmental Science

ORIGINAL RESEARCH
published: 04 November 2021
doi: 10.3389/fenvs.2021.780870

Property Risk Assessment of Sinkhole Hazard in Louisiana, U.S.A

Rubayet Bin Mostafiz[1]*, *Carol J. Friedland*[2], *Robert V. Rohli*[1,3] and *Nazla Bushra*[1]

[1]Department of Oceanography and Coastal Sciences, College of the Coast and Environment, Louisiana State University, Baton Rouge, LA, United States, [2]Bert S. Turner Department of Construction Management, Louisiana State University, Baton Rouge, LA, United States, [3]Coastal Studies Institute, Louisiana State University, Baton Rouge, LA, United States

Sinkholes (or dolines) are an often-overlooked environmental hazard. The processes that lead to their formation are slow and insidious, which encourage a lack of awareness or concern for the potential danger, until the sudden, climactic formation leads to unexpected property damage and possibly human casualties. This research identifies the risk to residential properties to the sinkhole hazard, using Louisiana, United States as a case study. Risk is defined as the product of the hazard intensity and the loss to structure and contents within the building resulting from the hazard-related disaster. Results suggest that risk is highly scale-dependent. Although the risk due to sinkholes is small on a per capita basis statewide, especially when compared to the per capita risk of other natural hazards, the property risk for census tracts or census blocks partially or completely overlying a salt dome is substantial. At finer scales, Terrebonne Parish, in coastal southeastern Louisiana, has the greatest concentration of salt domes, while Madison Parish, which is east of Monroe, has the highest percentage of area at risk for sinkhole formation, and St. Mary Parish—immediately west of Terrebonne—has the greatest risk of property loss. An Acadia Parish census tract has the maximum annual property losses in 2050 projected at $40,047 (2010$), and the highest projected annual per building ($43) and per capita ($18) property loss are in the same St. Mary Parish census tract. At the census block level, maximum annual property loss ($7,040) is projected for a census block within Cameron Parish, with maximum annual per building loss ($85 within West Baton Rouge Parish), and maximum per capita annual property loss ($120 within Plaquemines Parish). The method presented in this paper is developed generally, allowing application for risk assessment in other locations. The results generated by the methodology are important to local, state, and national emergency management efforts. Further, the general public of Louisiana, and other areas where the developed method is applied, may benefit by considering sinkhole risk when purchasing, remodeling, and insuring a property, including as a basis of comparison to the risk from other types of hazard.

Keywords: property loss, risk assessment, lake peigneur sinkhole, bayou corne sinkhole, napoleonville salt dome, Jefferson Island salt dome, doline, census block

OPEN ACCESS

Edited by:
Faik Bilgili,
Erciyes University, Turkey

Reviewed by:
Anzhelika Antipova,
University of Memphis, United States
Olaf Kühne,
University of Tübingen, Germany
Corinna Jenal,
University of Tübingen, Germany

***Correspondence:**
Rubayet Bin Mostafiz
rbinmo1@lsu.edu

Specialty section:
This article was submitted to Environmental Economics and Management, a section of the journal Frontiers in Environmental Science

Received: *21 September 2021*
Accepted: *06 October 2021*
Published: *04 November 2021*

Citation:
Mostafiz RB, Friedland CJ, Rohli RV and Bushra N (2021) Property Risk Assessment of Sinkhole Hazard in Louisiana, U.S.A. Front. Environ. Sci. 9:780870. doi: 10.3389/fenvs.2021.780870

INTRODUCTION

A sinkhole, also known as a doline, is a closed, circular surface depression on the landscape with no natural external surface drainage, caused by the abrupt or slow collapse of land by solution weathering. Sinkholes vary in size from a few square meters to hundreds of hectares, and extend from less than 1 m to over 30 m in depth. Sinkholes are most common in carbonate (i.e., limestone composed of calcite and less-commonly, dolostone composed of dolomite—karst environments), evaporite (i.e., composed of gypsum or halite), or other soluble rocks formed by the evaporation of water (Reynolds et al., 2021). Thus, sinkholes are most common in areas of limestone or with abundant salt domes (i.e., sedimentary rock structure caused by massive salt uplift, often trapping oil and/or natural gas), with rainy or formerly rainy climates, but humans can accelerate sinkhole formation. The majority of archival publications document how sinkholes provide unique niches for a wide array of bacteria (Wu et al., 2015), including large sulfur bacteria (e.g., Sharrar et al., 2017) and cyanobacteria (Biddanda et al., 2015), along with zooplankton (Montes-Ortiz and Elias-Gutierrez, 2018), and marine meiofaunal (Brankovits et al., 2021) communities, amphibians (Greenberg et al., 2015), and fossilized evidence of much larger animals (e.g., Shunk et al., 2009; Crowley and Godfrey, 2019), and form in interesting biogeochemical environments (e.g., Haas et al., 2018; Fazi et al., 2019). However, there is a dearth of research on economic losses due to sinkholes.

In recent years, radar has become the primary tool for identifying and understanding the evolution of sinkhole-caused surface deformation (Paine et al., 2012; Conway and Cook, 2013; Nof et al., 2013; Rucker et al., 2013; Caló et al., 2017; Szűcs et al., 2021). While prediction of the next sinkhole to form is extremely difficult even with many predictor variables (Orhan et al., 2020), there are recent signs that the next generations of synthetic aperture radar (Baer et al., 2018; Emil et al., 2021) and X-ray diffraction (Ghrefat et al., 2021) may offer advances over earlier radar technologies for early warning of sinkhole formation.

As development and property value continue to increase, sinkholes are a source of increasing property loss and human inconvenience and danger. While Louisiana, United States, is not usually considered to have a major sinkhole threat, from among the 153 known terrestrial salt domes in Louisiana (**Figure 1**) that have formed over the last 70 years, two sinkholes (Lake Peigneur in Jefferson Island salt dome in 1980 (Autin, 1984; **Figure 2A**) and Bayou Corne in the Napoleonville salt dome in 2012 (Louisiana Department of Natural Resources, 2012; Jones and Blom, 2014; **Figure 2B**) have formed, for a 0.025 percent annual probability of formation—a similar frequency as damaging earthquakes in western North America. These sinkholes were both precipitated by the human-influenced collapse of salt dome caverns, and both caused significant local and regional disruption. Other representative salt domes that have not yet produced sinkholes are shown in **Figures 2C,D**.

A more detailed understanding of sinkhole formation in Louisiana is needed to understand the threat more fully. Sinkholes in Louisiana are caused by the collapse of natural marine or terrestrial salt domes nearshore and offshore, typically by perforation, filling with water, and dissolution of the salts. The salt dome itself forms as a bed of evaporite rocks protrudes vertically upward, with a bubble-shaped interruption of other rock layers (Battelle Memorial Institute, 1981; Swann, 1989). These impermeable diapirs of salt are often sites of trapped oil and natural gas, which is common in Louisiana, as the state consistently ranks among the top U.S. states in hydrocarbon-based energy production. Thus, the perforation is often associated with oil/natural gas extraction.

In an early study, Johnson and Bredeson (1971) examined the structural history of six salt domes of south-central and southeastern Louisiana, suggesting that a core of salt or salt-shale combination underlies a sandstone and shale sequence, with folding and perhaps faulting playing a role in the emplacement of the shale in the core. Autin (2002) described the geologic features and evidence for uplift of the "Five Islands" salt domes of south-central and southwestern Louisiana, which includes two of the domes studied by Johnson and Bredeson (1971). Whyatt and Varley (2008) also explained the formation process of the sinkholes from the two domes in Louisiana. In light of this threat, the purpose of this research is to develop a method for estimating sinkhole risk, from statewide to the census-block level—the smallest geographic unit identified in the U.S. census—using Louisiana as an example.

FIGURE 1 | Terrestrial salt domes in Louisiana. Source: Derived from Beckman and Williamson (1990).

METHODS AND MATERIALS

Data

Latitude and longitude coordinates for salt dome centroids in Louisiana are gathered from Beckman and Williamson (1990),

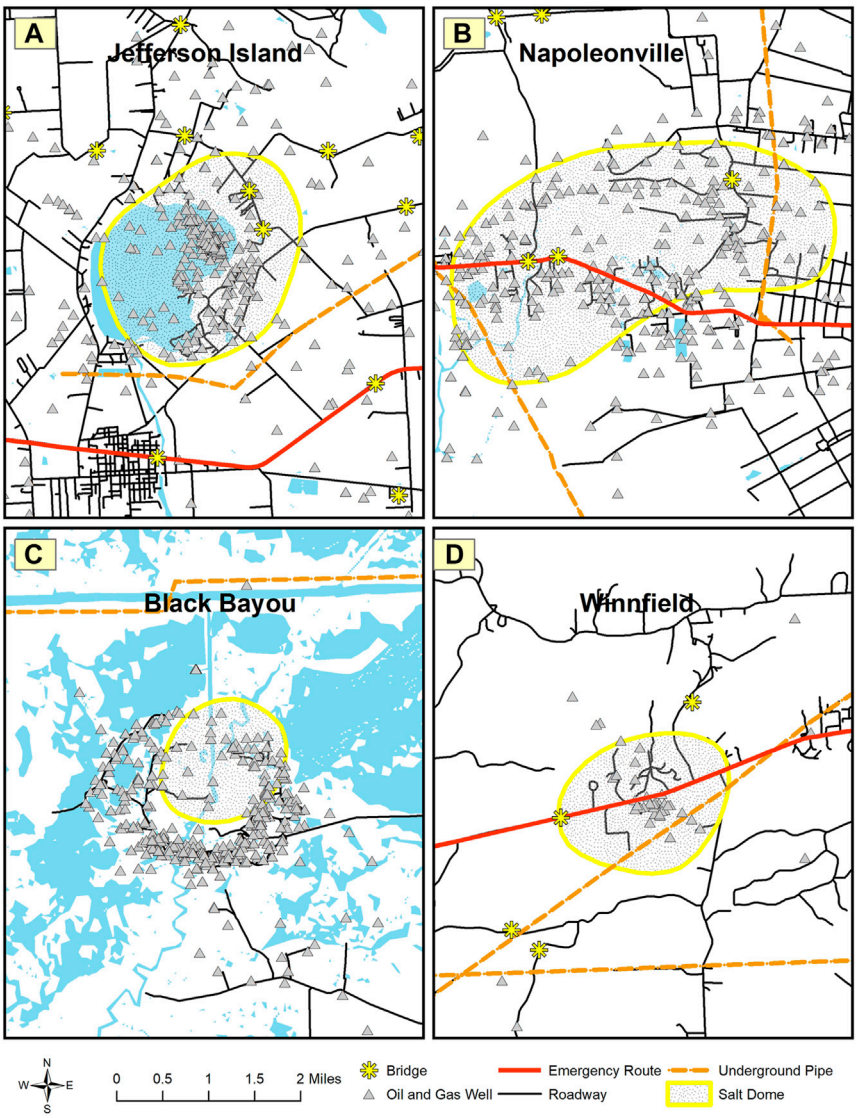

FIGURE 2 | Examples of notable salt domes in Louisiana, including the two that produced sinkholes, with nearby infrastructure: **(A)** Jefferson Island, Louisiana, salt dome with Lake Peigneur sinkhole designated; **(B)** Napoleonville, Louisiana, with Bayou Corne sinkhole located above a section of the Napoleonville salt dome; **(C)** Black Bayou, Louisiana, area, showing approximate salt dome location; and **(D)** Winnfield, Louisiana, area, showing approximate salt dome location. Source: Modified from Friedland et al. (2014).

from which shapefiles are created. The human component of the risk relies on Louisiana census-block shapefiles, which are downloadable from the U.S. Census Bureau (2010), and population projections based on data from U.S. Census Bureau (2020).

Methods

Historical Hazard Intensity

Of the 153 terrestrial salt domes in Louisiana, only Lake Peigneur and Bayou Corne became sinkholes from 1970 to present. Sinkholes before 1970 may be less likely to have been documented, particularly in rural areas. Thus, the probability since 1970 that a salt dome creates a sinkhole is 2/153 over a period of 52 years, for an annual formation probability of 2/(153*52), or 0.000251 (0.025 percent). The historical hazard intensity (annual probability that a salt dome will create a sinkhole; $H_{historical}$ is 0.00025. Offshore salt domes are not considered here.

Future Hazard Intensity

All indications are that the bedrock and regolith underlying Louisiana will not change on human timescales, and the relatively small percentage of Louisiana's land area composed of carbonate bedrock points to a continuing small hazard related to karst-induced sinkholes. Nevertheless, Autin (2002) emphasized that uplift of the Five Islands of southwestern

Louisiana is probably still active, leaving tectonic and geomorphic instability possible in the future, creating a cause for concern. Vulnerability to sinkholes could change much more rapidly with land use change and the pressures of increased resource extraction and population growth. Sinkhole risk could also increase as a "side effect" to changes in the vulnerability to other hazards. For example, sea level rise contributes to saltwater intrusion, which contributes to the formation of salt domes, which—when mined extensively—can form sinkholes.

Despite the fact that geological changes are unlikely, other environmental modifications are connected with changes in sinkhole formation, including, according to Demir and Keskin (2020), anthropogenic effects. Nevertheless, it is important to note that geological factors such as groundwater leakage rates (i.e., Xiao and Li, 2020) may also be important indicators of sinkhole formation, independent of climate change considerations. Sedimentation in sinkholes has also been used as an indicator of climate and sea level change (Hodell et al., 2005; van Hengstum et al., 2011; Kovacs et al., 2013; Gregory et al., 2017; Peros et al., 2017; Farley et al., 2018). Taminskas and Marcinkevicius (2002) pointed out that climate change may drive karstification that then in turn affects sinkhole formation. Panno et al. (2012) noticed that cave formation was affected by climate change in the Pleistocene. Linares et al. (2017) found that drought facilitates sinkhole formation in some karst settings, including northeastern Spain. Most recently, biological manifestations of climate change in sinkholes have been shown for vascular plants (Bátori et al., 2014; Kiss et al., 2020), bryophytes (Liu et al., 2019), and forests (Yang et al., 2019).

In light of the above factors, the annual probability estimate [i.e., future hazard intensity (H_{2050})] for areas overlying a salt dome is likely to increase somewhat by 2050. This is because likely increasing population (and therefore, it is assumed, groundwater pumping) and human activities (including resource extraction, possibly from hydraulic fracture drilling), along with the destabilizing effects of global and regional sea level rise on coastal salt domes, are increasingly likely to generate additional accidental events. In light of these considerations, the hazard intensity (i.e., a sinkhole forms from a salt dome) is assumed here to increase by 50 percent by 2050 from $H_{historical}$, for a multiplication factor (F_{2050}) of 1.5 for the sinkhole hazard (i.e., $H_{2050} = H_{historical} x\, F_{2050}$). Yet there is wide uncertainty in the precise increase in exposure to the hazard. Thus, a sensitivity analysis is undertaken here to ascertain the property risk under scenarios of F_{2050} of sinkholes in Louisiana by 2050, with H_{2050} ranging from 0.0250 (low scenario; equal to $H_{historical}$) to 0.0375 (medium scenario) to 0.0500 percent (high scenario, i.e. F_{2050} = 1.00, 1.50, and 2.00).

Population Projection

Because property risk requires knowledge of not only $H_{historical}$ and F_{2050}, but also the exposure to the hazard, population (P) projection is necessary. The technique for P projection follows that of Mostafiz et al. (2020a). Specifically, annual P growth rate is calculated here at the county (or "parish" in Louisiana; j) scale because the U.S. Census Bureau does not estimate annual P by census tract or census block (i). The mean of the annual (i.e., from 1 year to the next) P growth rate (r_j) for the n-year period (i.e., from 1980–2020 in this analysis) is computed, beginning in year y (i.e., 1980 here) as described by **Eq. 1**:

$$r_j = \frac{\sum_{y}^{y+n}\left[\frac{(P_{j,y+1}-P_{j,y})}{P_{j,y}}\right]}{n} \quad (1)$$

After r_j is calculated for each of Louisiana's 64 parishes, future P change is downscaled to the census block (i), assuming that r_j remains constant for each census block in a given parish. Next, future P is estimated by census block, assuming that unpopulated census blocks in 2010 remain unpopulated through 2050. This projection is done by using the 2010 P for each i as the base (i.e., $P_{0,i} = P_{2010,i}$). In this manner, future (f) P is estimated to 2050 (i.e., $P_{f,i} = P_{2050,i}$), given a n (or t)- year period of P change, as depicted by the continuously compounding growth equation in **Eq. 2**:

$$P_{f,i} = P_{0,i}e^{r_j\, t} \quad (2)$$

Other methods for estimating P change in similar research have been considered (Mostafiz et al., 2020a). For example, projection of a regression-based trendline for each parish P to 2050 and extrapolation of the growth rate trendline for P projection in 2050 are both inappropriate, owing to small explained variance and insignificance of the trendlines in some cases. It is likely that one or both of these approaches failed because of large, abrupt, and temporary P changes within and beyond Louisiana in the aftermath of hurricanes (most notably Katrina in 2005, and perhaps Laura in 2020 and Ida in 2021). By contrast, the technique undertaken herein has been found to be optimal in the absence of official demographic projections, as it was found to be least sensitive to these issues (Mostafiz et al., 2021a; Mostafiz et al., 2021b).

Assessing Building/Structure and Content Value

Similar to Mostafiz et al. (2021a), Mostafiz et al. (2021b), current and future building/structure value (SV) are evaluated by census block, assuming that only the inhabited areas have residential or commercial property value. U.S. Census Bureau (2010) is used to count the buildings by census block in 2010 ($N_{2010,i}$) by summing the existing buildings listed in the shapefiles as having been completed during each time interval. Then, N in 2010 is multiplied by the mean SV in 2010, by census block ($AV_{2010,i}$), to approximate the total SV by census block ($SV_{2010,i}$), as shown in **Eq. 3**:

$$SV_{2010,i} = N_{2010,i} \times AV_{2010,i} \quad (3)$$

The building count in 2050 by census block ($N_{2050,i}$) is assumed to change in proportion to population of the parish in which that census block is located. Thus, the P projection methodology described in the previous subsection is used to estimate SV in 2050. Total SV by census block in 2050 ($SV_{2050,i}$) is computed as the product of the total SV in 2010 and the ratio of P in 2050 vs. 2010 by census block, as described in **Eq. 4**:

$$SV_{2050,i} = SV_{2010,i} \times \frac{P_{2050,i}}{P_{2010,i}} \quad (4)$$

In addition to these methods used by Mostafiz et al. (2021a), Mostafiz et al. (2021b), here not only must *SV* be considered, but also the content value (*CV*), which includes the goods, but not services, included on the damaged property. In National Structure Inventory (NSI) 2.0 (United States Army Corps of Engineers, 2019), *CV* is calculated by multiplying *S* by an occupancy-type-specific structure-to-content value ratio. Residential structures in NSI 2.0 (USACE, 2019) are assumed to have *CV* equal to *SV*, and *CV* is assumed to be half of *SV* in cases for which the USACE economic guidance memorandum depth-damage functions are not used. Moreover, NSI 2.0 (USACE 2019) recommends the assumption that *CV* equals *SV* for commercial and industrial facilities, which are more likely to contain expensive and abundant equipment and merchandise. By contrast, Hazus (FEMA 2013, pp. 6–9) recommends assuming that *CV* is half of *SV* for residential structures. Despite the fact that this research includes only residential buildings and most Louisianians do not live an opulent lifestyle that includes expensive jewelry and other such possessions, the nature of the sinkhole hazard is such that vehicles, boats, tool sheds, and other outdoor possessions over a forming sinkhole would be lost in addition to indoor possessions. For all these reasons, as shown in **Eq. 5**, it is assumed that:

$$CV = 0.75\,SV \quad (5)$$

The property value (*PV*) is the sum of *SV* and *CV*.

Projecting Future Property Loss

Estimation of future property loss begins with estimating surface areas on or near salt domes. Although the centroids and diameters of 78 of the 153 terrestrial Louisiana salt domes are known and range from 0.13 to 2 mi (Beckman and Williamson, 1990), salt dome areas are unavailable and areas must be derived by assuming circularity of all salt domes. Where salt dome diameters are unknown, the diameter is assumed to equal that of the largest known salt dome diameter. Although it provides a conservative estimate of loss, this assumption is justified because it is likely that some terrestrial Louisiana salt domes may not have been mapped completely to date. The largest terrestrial salt domes in the state with known dimensions (i.e., Bayou Choctaw, Chacahoula, Napoleonville, South Tigre Lagoon, and Stella; in Iberville, Lafourche, Assumption, Iberia, and Plaquemines parishes, respectively) each have an estimated diameter of 2 mi (i.e., no additional significant digits provided; surface area of 3.14 mi^2; Beckman and Williamson, 1990). To derive salt dome areas, a circle is drawn from the salt dome centroid to its radius.

The next step in estimating future property loss is to derive estimates of the sinkhole areas. The two sinkholes (Lake Peigneur and Bayou Corne) have known surface areas of 1.76 (FTN Associates, Ltd., 2002) and only 0.06 mi^2 (Clapp, 2018), respectively. Again, a conservative estimate is used, as it is assumed that future sinkholes will be of the area of the larger of the two known sinkholes. This procedure is justified by the assumption that human impacts on salt domes will increase over time.

Future property loss estimates must then be treated separately for property located on top of the sinkhole vs. property on a salt dome but not in a sinkhole. To estimate loss for property located atop a sinkhole, the ratio of the area of the larger sinkhole to the largest salt dome (*R*) is 1.76/3.14, or 0.56. A 100 percent loss (i.e., L_A= 1.00) of *SV* and *CV* is assumed to occur across the 56 percent of the area of a salt dome that produces a sinkhole. In the remaining 44 percent of the salt dome surface area (i.e., property on the salt dome but not the sinkhole—the periphery of the sinkhole), a loss of 50 percent (i.e., L_B= 0.50) of *SV* and no loss of *CV* is assumed. The rationale for a 50 percent loss of *SV* is based on the assumption that structures on the salt dome but not the sinkhole will only suffer partial damage. The neglected loss of *CV* is based on the assumption that homeowners will have been alerted of an imminent sinkhole hazard and will have moved their valuable possessions, including vehicles, immediately upon formation of the core of the sinkhole, and/or the unmoved contents will not fall into the sinkhole. The map of Louisiana census blocks, is then overlaid upon the salt dome areas. The "tabulate intersection" tool in ArcGIS® is used to compute the proportion (percent) of a census block that lies over the salt dome for each census block (A_i).

The estimated structure loss by 2050 in a census block ($SL_{2050,i}$) over a salt dome (i.e., over or near a sinkhole) is shown by **Eq. 6**:

$$SL_{2050,i} = \left(SV_{2050,\,i} \times A_i \times H_{historical} \times F_{2050}\right)[R \times L_A + (1 - R) \times L_B] \quad (6)$$

Equation 6 quantifies the two components of structure loss in a given census block: for locations in which the sinkhole overlaps a salt dome, and for locations within a salt dome but not a sinkhole. Census blocks that overlie neither a salt dome nor a sinkhole will have $A_i = 0$ and therefore are assigned zero *SL* and zero risk.

Likewise, the estimated content loss ($CL_{2050,i}$) is calculated as shown in **Eq. 7**:

$$CL_{2050,i} = CV_{2050,\,i} \times A_i \times H_{historical} \times F_{2050} \times R \times L_A \quad (7)$$

Equation 7 verifies that there is no *CL* for parts of the census track that overlie a salt dome but are not in a sinkhole (i.e., there is no L_B term). All losses are expressed in 2010$. Historical (present) structure loss ($SL_{2021,i}$) is calculated using $SV_{2010,\,i}$, A_i, $H_{historical}$, *R*, L_A, and L_B. Similarly, the historical (present) content loss ($CL_{2021,i}$) is computed from $CV_{2010,\,i}$, A_i, $H_{historical}$ *R*, and L_A. Property loss (*PL*) is the sum of *SL* and *CL*.

RESULTS

Hazard Intensity

A total of 0.55 percent of Louisiana's area is over a terrestrial salt dome, with 36 of Louisiana's 64 parishes (56.25 percent) partially over a salt dome and 28 (43.75 percent) totally unassociated with a salt dome. Terrebonne Parish, which includes Houma (**Figure 1**), has the most terrestrial salt domes (16), with 1.36 percent of its area lying over a salt dome. Madison, which is east

of Monroe along the Mississippi River, is the most vulnerable parish in terms of formation of future sinkholes, where 2.73 percent of the area overlies salt domes.

At a finer scale, a total of 93 of the state's 1,148 census tracts (8.10 percent) are partially over a salt dome and 1,055 (91.90 percent) are totally unassociated with a salt dome. Census tract 22101041500 in St. Mary Parish, which lies immediately to the west of Terrebonne, is the most vulnerable in terms of formation of future sinkholes, where 86.57 percent of its area overlies a salt dome. At an even finer scale, 1,064 (0.52 percent) of the state's census blocks completely overlie a salt dome, with 1,138 (0.56 percent) partially and 201,245 (98.92 percent) totally unassociated with a salt dome. Thus, only 2,202 census blocks (1.08 percent in the state) lie completely or partially on a salt dome.

Population Projection

The population rate values identified in **Eqs 1**, **2** allow for the projection of *P* and its change since 2010. It is assumed that the 102,781 unpopulated census blocks in 2010 from among the 203,447 total in Louisiana remain uninhabited along with 37 census blocks that were so sparsely populated in 2010 that they are projected to be unpopulated (i.e., have a *P* less than 1) by 2050. Thus, 100,629 census blocks are projected to be populated and 102,818 are projected to be unpopulated by 2050.

Louisiana's population in 2010 is greatest around the four largest metropolitan areas of New Orleans, Baton Rouge, Shreveport-Bossier City, and Lafayette (**Figure 3A**). Increases by 2050 will be greatest in the same general areas, but with particularly strong increases near Lafayette, Baton Rouge, and in the "Florida" parishes of east-central Louisiana, east of Baton Rouge (**Figure 3B**). Decreased population by 2050 is projected in northeastern Louisiana, along the Red River Valley from Shreveport to the area southeast of Alexandria, the New Orleans area, east of Lake Charles, and various other scattered locations (**Figure 3B**). **Supplementary Appendix SA** shows these values by parish.

Of the 2,202 census blocks under risk of sinkhole formation (i.e., overlying or partially overlying a salt dome), only 900 were populated in 2010; all of these are projected to be populated in 2050. Of these 900, 222 (0.11 percent) lie completely over and 678 (0.33 percent) partially overlap a salt dome. The remaining 202,547 (99.56 percent) are totally unassociated with a salt dome.

Structure and Content Value

The *SV* identified in **Eqs 3**, **4**, and the *CV* calculated in **Eq. 5** allow for the projected SV_{2050}, CV_{2050}, and their change since 2010. Not surprisingly, property value is concentrated around the largest metropolitan areas of New Orleans, Baton Rouge, Shreveport-Bossier City, and Lafayette (**Figure 4A**). By 2050, property value will be greatest in the same general areas, but with particularly strong increases near Lafayette, Baton Rouge, and in the Florida parishes of east-central Louisiana, east of Baton Rouge (**Figure 4B**). Areas of decreased property values in 2050 generally overlap with areas of projected decreases in population by 2050 (compare **Figure 4B** to **Figure 3B**). **Supplementary Appendix SA** shows these values by parish.

At the statewide level, the historical (present) average annual property (structure + content) loss due to sinkhole is $211,283 (2010$), while the historical average annual per building property loss was $0.11 and the historical average annual per capita property loss due to sinkhole is only $0.047 (2010$; **Supplementary Appendix SB**) for this localized hazard. Expanding oil and natural gas exploration may potentially increase the sinkhole risk by 2050 as population, development, and the pressures of climate change, and therefore annual property loss (structure + content) due to sinkhole, increase. The 2050-projected annual property loss is $310,734 (2010$), an increase of 47.07 percent (**Table 1** and **Supplementary Appendix SB**). Even though *CV* is assumed to be 75 percent of *SV* over the salt dome, the totals in **Table 1** reflect a smaller percentage of *CL* relative to *SL* because no content is assumed to be lost in areas on the fringes of the salt dome. Annual per building and per capita property losses are projected to remain small by 2050, though larger than the historical (present) values. The projected per building loss is estimated as $0.13 (**Supplementary Appendix SB**), an increase by 20 percent. Projected per capita property loss is $0.055 by 2050, an increase of 18 percent (**Supplementary Appendix SB**). Still, however, per capita losses are projected to be very small when viewed on a statewide basis.

The distribution of losses is expected to remain similar to present dominant areas (**Figures 5A,B**). The coastal and northeastern Louisiana parishes where salt domes are most concentrated are the areas with the most risk. At the parish level, St. Mary has the highest historical (present) overall sinkhole annual property risk ($58,782), while sparsely-populated Cameron Parish in extreme southwestern Louisiana has the highest present annual per building property loss ($4.06) and per capita property loss ($2.14) due to the sinkhole hazard (**Supplementary Appendix SB**). Despite the fact that changes in the sinkhole probability and expansion of population are projected to change the sinkhole risk by 2050, the greatest annual sinkhole property loss ($66,199) is expected to remain in St. Mary Parish. Likewise, annual per building property loss ($6.22) and per capita property loss ($3.20) are expected to remain in Cameron Parish (**Supplementary Appendix SB**).

Census tract 22101041500 in St. Mary Parish has the highest historical (present) mean annual property (structure + content) loss ($24,545), the largest historical mean annual per building property loss ($28.74), and the greatest historical annual per capita property loss ($12.33) in the state due to the sinkhole hazard. By 2050, the highest annual mean property loss (structure + content) due to a sinkhole ($40,047) is projected to be in census tract 22,001,960,700, in Acadia Parish of southwestern Louisiana, immediately west of Lafayette Parish. However, the greatest annual per building property loss ($43.08) and the highest annual per capita property loss ($18.34) will remain in the same St. Mary census tract described above.

At the finer census-block level, the greatest historical (present) mean annual property loss ($6,140) is in census block 220,239,701,005,040 of Cameron Parish. The highest historical

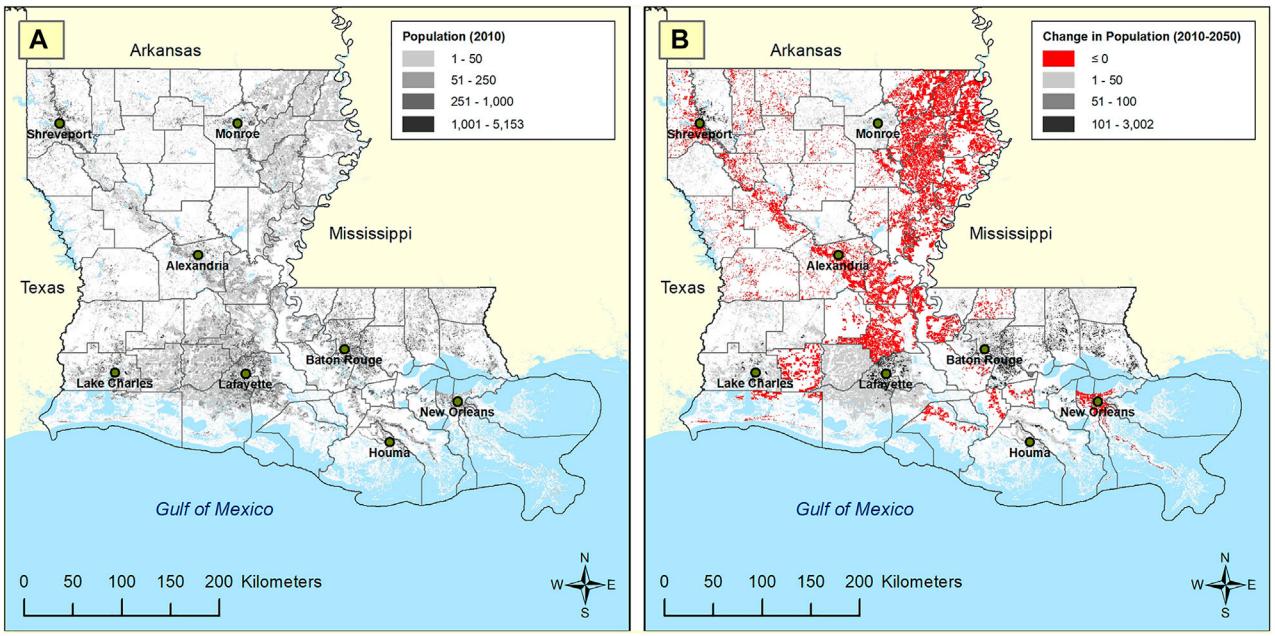

FIGURE 3 | Population by census block: **(A)** 2010, and **(B)** change in population from 2010 to 2050. Source: Mostafiz et al. (2021a), Mostafiz et al. (2021b).

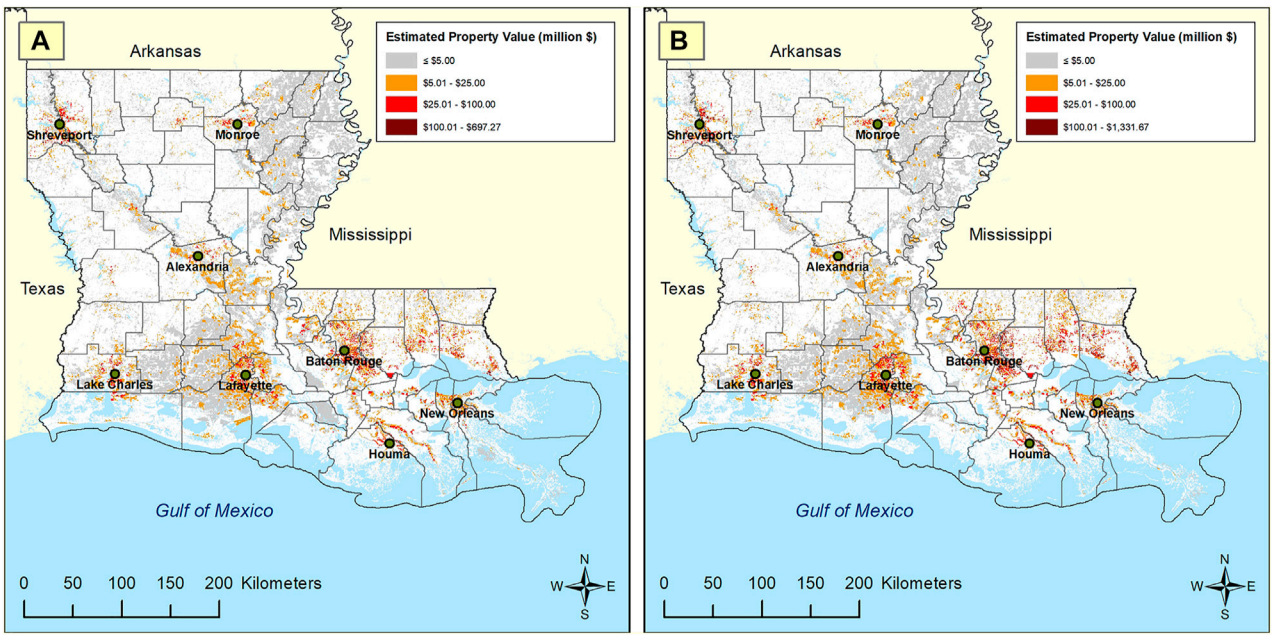

FIGURE 4 | Estimated property value by census block (structure + content, 2010$): **(A)** 2010, and **(B)** 2050. Historical (Present) and Projected Property Loss.

mean annual per building property loss ($56.37) is in census block 221,210,203,001,115, in West Baton Rouge Parish (immediately west of Baton Rouge). The greatest historical annual per capita property loss in the state is $80.19 in census block 220,750,501,002,010, in Plaquemines Parish (at the birdfoot delta of the Mississippi River). By 2050, the highest annual property loss (structure + content) due to a sinkhole ($7,050) is projected to remain in the same Cameron Parish census block. The largest annual per building property loss ($84.56) will remain in the same West Baton Rouge census block. And likewise, the greatest annual per capita property loss ($120.29) is projected to continue to be the same Plaquemines Parish census block.

TABLE 1 | Comparison of Louisiana statewide property loss: Historical (present) vs. 2050-projected; All represent a 47.07 percent increase by 2050.

Property	Historical (present) average annual loss (2010$)	Projected average annual loss in 2050 (2010$)
Structure	$137,334	$201,977
Content	$73,949	$108,757
Total	$211,283	$310,734

Sensitivity Analysis

The sensitivity analysis demonstrates the impact of model assumptions regarding F_{2050}, *SV* to *CV* ratio, and *R* (**Table 2**). If the assumption that the hazard does not change from the present (i.e., F_{2050} =1, for a zero percent change) or the hazard intensity doubles (i.e., F_{2050} = 2, for a 100 percent increase) by 2050, rather than the 50 percent increase (i.e., F_{2050} =1.5) currently assumed, the result changes by 33 percent (**Table 2**).

If *CV* would be taken to be only half of *SV* or equal to *SV*, instead of three-quarters of *SV*, the sensitivity is below 12 percent (**Table 2**). However, the greatest sensitivity in model assumptions is that for *R*, which is derived as the ratio of the larger sinkhole to the largest salt dome (0.56). If *R* would have instead been derived such that the sinkhole is equal in area to the salt dome, then *R* would have been 1.0, or 0.44 larger than the modeled assumption. Taking ±0.44 from this 0.56 in the low and high scenarios would cause the annual loss in 2050 to change by almost 46 percent (**Table 2**).

DISCUSSION

Although the total loss from the sinkhole hazard is small compared to losses due to other Louisiana hazards, such as extreme heat and cold (Mostafiz et al., 2020a; 2020b), expansive soils (Mostafiz et al., 2021a), wildfire (Mostafiz et al., 2021b), and flood (Mostafiz et al., 2021c; 2021d), these losses are nevertheless important to document as part of a complete hazard mitigation plan. Furthermore, the localized nature of this hazard, in contrast to others, which are statewide problems, causes the calculation of a statewide mean per capita loss to appear small. However, mean loss reveals little for the sinkhole hazard because losses are likely to be exorbitant for those affected while others remain unaffected. In that respect, these results resemble those for hail, lightning, and tornadoes in Louisiana (Mostafiz et al., 2020a; 2020b), although the risk for sinkholes is even lower than that for these hazards. Additionally, sinkhole is different from the other hazards analyzed because homeowners near or over a salt dome know the risk, and others need not consider the risk. By contrast, losses from other natural hazards in Louisiana are more random and widespread across the state. The results for sinkholes are perhaps even more highly dependent on scale than the results for other hazards, which is unfortunate because often the scale of analysis does not match the scale of the hazard being analyzed. This is an important point because mitigation planning efforts are often focused on the parishwide or even statewide scale, yet the hazard exists only at the much more localized scale.

Future changes to the sinkhole hazard in Louisiana will be influenced by the spatial relationship between population growth and salt domes. Future population and property value are projected to increase in the Florida parishes where there are no salt domes (**Figures 1, 3B, 4B**). Most salt domes are in coastal areas where population and property value are decreasing at the census block level. These results are

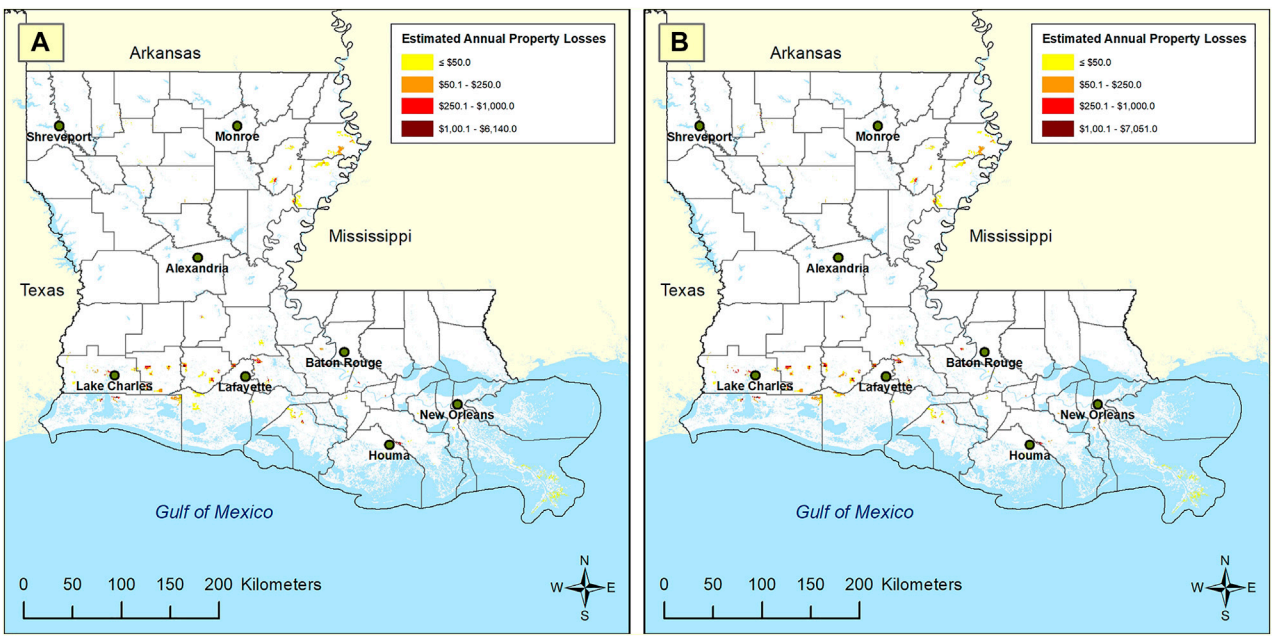

FIGURE 5 | Estimated annual property loss (2010$) due to sinkhole by census block: **(A)** historical (present), and **(B)** 2050.

TABLE 2 | Sensitivity analysis of 2050 projections of Louisiana statewide annual property loss (i.e., risk) due to sinkhole, by parameter (2010$).

Parameter	Low Scenario	Modeled (Eqs 6 + 7)	High Scenario	Difference from Eqs 6 + 7 (%)
Future Condition (F_{2050})	$207,155 (+0%)	$310,734 (+50%)	$414,311 (+100%)	±33.3
Content to Structure Value Ratio (*CV*/*SV*)	$274,481 (*CV* = 0.5 *SV*)	$310,734 (*CV* = 0.75 *SV*)	$346,986 *CV* = *SV*	±11.7
Sinkhole to Salt Dome Ratio (*R*)	$168,314 (*R* = 0.12)	$310,734 (*R* = 0.56)	$453,152 (*R* = 1.00)	±45.8

important not only as part of a disaster preparation and mitigation program, but also for actuarial and real estate interests. This information also assists in evaluating comprehensively the benefits vs. cost of human activities in the environment.

LIMITATIONS

The results rest on the three major assumptions described in **Table 2**. Specifically, these include estimates of the changing hazard intensity, the *CV*/*SV* ratio, and the geometry of salt domes and the percentage of salt domes that become sinkholes, albeit based on only two historical sinkhole occurrences. Caution should also be exercised in the interpretation of results because identification of which portion/part of salt domes will turn into sinkholes is highly uncertain. The sensitivity analysis is performed to provide a range of outputs in light of these uncertainties, so that future users can benefit from this research after the future hazard becomes more certain, more accurate estimates of *CV*/*SV* become available for this area, and/or the accurate dimension or areal extent of salt domes and sinkholes are mapped.

SUMMARY AND CONCLUSION

This research represents a first attempt to assess the historical (present) and future (i.e., 2050) economic risk to property due to the sinkhole hazard in Louisiana, using a set of basic assumptions. For instance, an increase in hazard intensity of 50 percent from present levels is assumed, based on expected increases in population, development, mineral extraction, and the pressures of climate change. The ratio of content value to structure value in the hazard area is assumed to be 0.75, with adjustments made for locations above vs. near the salt dome. It is also assumed here that salt domes and sinkholes are both circular, and that losses are concentrated over the sinkhole itself, with the ratio of the largest sinkhole incident area in Louisiana to the largest salt dome area used to calculate the losses. Despite the assumptions, the results are valuable and represent an important component of a comprehensive hazard planning, mitigation, and management program, and to serve actuarial and real estate interests. The generalized nature of the method presented here allows for application of risk assessment in other locations.

In general, results suggest that the risk of sinkholes is small on a per building and capita basis statewide, especially when compared to the per capita risk of other natural hazards. However, the property risk for census tracts and (especially) census blocks partially or completely overlying a salt dome is substantial. Terrebonne Parish, in coastal southeastern Louisiana, has the greatest concentration of salt domes, while Madison Parish, which is east of Monroe along the Mississippi River in northeastern Louisiana, has the highest percentage of area under sinkhole risk, and St. Mary Parish—immediately west of Terrebonne—has the greatest risk of property loss. Current and future risk to annual property loss, per building loss, and per capita property loss are maximum in a St. Mary Parish census tract, excepting that a census tract in Acadia Parish is projected to have the highest mean annual property loss by 2050, from among Louisiana's 1,148 census tracts. At an even finer scale, one particular census block in each of Cameron, West Baton Rouge, and Plaquemines parishes presently have and are projected to continue to have the maximum annual property losses, per building property losses, and per capita property losses, respectively, from among Louisiana's 203,447 census blocks by 2050.

Inasmuch as the increasing pressures of increased population appear to be inevitable, vulnerability to sinkholes appears to be increasing. Therefore, future research is needed to better identify the precise location of both the salt domes and sinkholes, so that a more precise and accurate overlay on the demographic variables (i.e., population and projected population) can be used to assign risk. Moreover, more elaborate population and other demographic projections, such as average income or poverty quotients, in the affected areas would improve estimates of the extent of loss for those affected, especially at finer spatial resolutions. Research on the losses incurred on property adjacent to sinkholes is also needed to improve loss projections. Finally, technological advancements may allow future prediction of sinkholes, which would minimize not only economic losses, but also losses to human life.

DATA AVAILABILITY STATEMENT

The original contributions presented in the study are included in the article/**Supplementary Material**, further inquiries can be directed to the corresponding author.

AUTHOR CONTRIBUTIONS

RM developed the detailed methodology, collected and analyzed the data, and developed the initial text. CF conceptualized the hazard quantification and revised the text. RR developed the future projection of sinkhole hazard and edited early and late drafts of the text. NB provided oversight on analysis, particularly regarding the population projections, and revised the text.

FUNDING

This project resulted from the 2019 Louisiana State Hazard Mitigation Plan update, for which CF and RR received funding from FEMA, *via* GOHSEP, grant number: 2000301135. Any opinions, findings, conclusions, and recommendations expressed in this manuscript are those of the authors and do not necessarily reflect the views of FEMA or GOHSEP. Publication of this article was subsidized by the Louisiana State University (LSU) Libraries Open Access Author Fund and the Performance Contractors Professorship in the College of Engineering at LSU.

ACKNOWLEDGMENTS

The authors warmly appreciate the overall project support from Jeffrey Giering of Louisiana's Governor's Office of Homeland Security and Emergency Preparedness (GOHSEP).

SUPPLEMENTARY MATERIAL

The Supplementary Material for this article can be found online at: https://www.frontiersin.org/articles/10.3389/fenvs.2021.780870/full#supplementary-material

REFERENCES

Autin, W. J. (1984). "Geologic significance of land subsidence at Jefferson Island, Louisiana," in *Gulf Coast Association of Geological Societies Transactions*, 34, 293–309. Available at:. doi:10.1306/a1addb10-0dfe-11d7-8641000102c1865d https://archives.datapages.com/data/gcags/data/034/034001/0293.htm (Last accessed: October 11, 2021)

Autin, W. J. (2002). Landscape evolution of the Five Islands of south Louisiana: Scientific policy and salt dome utilization and management. *Geomorphology* 47 (2–4), 227–244. doi:10.1016/S0169-555X(02)00086-7

Baer, G., Magen, Y., Nof, R. N., Raz, E., Lyakhovsky, V., and Shalev, E. (2018). InSAR measurements and viscoelastic modeling of sinkhole precursory subsidence: Implications for sinkhole formation, early warning, and sediment properties. *J. Geophys. Res. Earth Surf.* 123 (4), 678–693. doi:10.1002/2017JF004594

Bátori, Z., Csiky, J., Farkas, T., Vojtkó, A., Erdős, L., Kovács, D., et al. (2014). The conservation value of karst dolines for vascular plants in woodland habitats of Hungary: refugia and climate change. *Ijs* 43 (1), 15–26. doi:10.5038/1827-806X.43.1.2

Battelle Memorial Institute (1981). *Geologic Evaluation of Gulf Coast Salt Domes: Overall Assessment of the Gulf Interior Region (ONWI-106)*. Columbus. Available at: https://inis.iaea.org/search/search.aspx?orig_q=RN:14733847 (Last accessed October 11, 2021). OH (U.S.A.) Office of Nuclear Waste Isolation

Beckman, J. D., and Williamson, A. K. (1990). Salt-dome locations in the Gulf Coastal Plain, South-Central United States. *U.S. Geol. Surv.* Vol. 90, 4060. doi:10.3133/wri904060

Biddanda, B. A., McMillan, A. C., Long, S. A., Snider, M. J., and Weinke, A. D. (2015). Seeking sunlight: rapid phototactic motility of filamentous mat-forming cyanobacteria optimize photosynthesis and enhance carbon burial in Lake Huron's submerged sinkholes. *Front. Microbiol.* 6, 930. doi:10.3389/fmicb.2015.00930

Brankovits, D., Little, S. N., Winkler, T. S., Tamalavage, A. E., Mejía-Ortíz, L. M., Maupin, C. R., et al. (2021). Changes in organic matter deposition can impact benthic marine meiofauna in karst subterranean estuaries. *Front. Environ. Sci.* 9, 157. doi:10.3389/fenvs.2021.670914

Caló, F., Notti, D., Galve, J., Abdikan, S., Görüm, T., Pepe, A., et al. (2017). Dinsar-based detection of land subsidence and correlation with groundwater depletion in Konya Plain, Turkey. *Remote Sensing* 9 (1), 83. doi:10.3390/rs9010083

Clapp, J. (2018). Documentary looks at community impact of Bayou Corne sinkhole. *The Advocate* (Baton Rouge). Available at: https://www.houmatoday.com/news/20181012/documentary-looks-at-community-impact-of-bayou-corne-sinkhole (Last accessed October 11, 2021).

Conway, B. D., and Cook, J. P. (2013). "Monitoring evaporite karst activity and land subsidence in the Holbrook Basin, Arizona using interferometric synthetic aperture radar (InSAR)," in *Proceedings of the Thirteenth Multidisciplinary Conference on Sinkholes and the Engineering and Environmental Impacts of Karst. Carlsbad* (New Mexico: National Cave and Karst Research Institute). 187–194. doi:10.5038/9780979542275.1126

Crowley, B. E., and Godfrey, L. R. (2019). Strontium isotopes support small home ranges for extinct lemurs. *Front. Ecol. Evol.* 7, 490. doi:10.3389/fevo.2019.00490

Demir, V., and Keskin, A. Ü. (2020). Water level change of lakes and sinkholes in Central Turkey under anthropogenic effects. *Theor. Appl. Climatol* 142 (3), 929–943. doi:10.1007/s00704-020-03347-5

Emil, M. K., Sultan, M., Alakhras, K., Sataer, G., Gozi, S., Al-Marri, M., et al. (2021). Countrywide monitoring of ground deformation using InSAR time series: A case study from Qatar. *Remote Sensing* 13 (4), 702. doi:10.3390/rs13040702

Farley, G., Schneider, L., Clark, G., and Haberle, S. G. (2018). A Late Holocene palaeoenvironmental reconstruction of Ulong Island, Palau, from starch grain, charcoal, and geochemistry analyses. *J. Archaeological Sci. Rep.* 22, 248–256. doi:10.1016/j.jasrep.2018.09.024

Fazi, S., Ungaro, F., Venturi, S., Vimercati, L., Cruz Viggi, C., Baronti, S., et al. (2019). Microbiomes in soils exposed to naturally high concentrations of CO2 (Bossoleto Mofette Tuscany, Italy). *Front. Microbiol.* 10, 2238. doi:10.3389/fmicb.2019.02238

FEMA (2013). *Multi-hazard Loss Estimation Methodology, Flood Model, Hazus-MH, User Manual*. Washington DC. Available at: https://www.fema.gov/sites/default/files/2020-09/fema_hazus_flood-model_user-manual_2.1.pdf (Last accessed October 11, 2021).

Friedland, C. J., Joyner, T. A., Mecholsky, K. M., Rohli, R. V., Gilliland, J., Madani, S. A., et al. (2014). State of Louisiana Hazard Mitigation Plan: 2014 Update. *For Governor's Office of Homeland Security and Emergency Preparedness*, 637. Available at: http://gohsep.la.gov/Portals/0/Documents/Mitigate/SHMPU_2014.pdf (Last accessed October 11, 2021).

FTN Associates, Ltd (2002). Lake Peigneur TMDLS for dissolved oxygen and nutrients. Available at: https://web.archive.org/web/20150924143856/https://www.epa.gov/waters/tmdldocs/FTNLakePeigneur.pdf (Last accessed October 11, 2021).

Ghrefat, H., Hakami, A., Ibrahim, E., Mogren, S., Qaysi, S., Abdelrahman, K., et al. (2021). Damage assessment of a salt dome in Jizan, southwestern Saudi Arabia, using high spatial resolution remote sensing data. *Front. Earth Sci.* 9. doi:10.3389/feart.2021.700337

Greenberg, C. H., Goodrick, S., Austin, J. D., and Parresol, B. R. (2015). Hydroregime prediction models for ephemeral groundwater-driven sinkhole wetlands: A planning tool for climate change and amphibian conservation. *Wetlands* 35 (5), 899–911. doi:10.1007/s13157-015-0680-0

Gregory, B. R. B., Reinhardt, E. G., and Gifford, J. A. (2017). The influence of morphology on sinkhole sedimentation at Little Salt Spring, Florida. *J. Coastal Res.* 332 (2), 359–371. doi:10.2112/JCOASTRES-D-15-00169.1

Haas, S., De Beer, D., Klatt, J. M., Fink, A., Rench, R. M., Hamilton, T. L., et al. (2018). Low-light anoxygenic photosynthesis and Fe-S-biogeochemistry in a microbial mat. *Front. Microbiol.* 9, 858. doi:10.3389/fmicb.2018.00858

Hodell, D. A., Brenner, M., Curtis, J. H., Medina-González, R., Ildefonso-Chan Can, E., Albornaz-Pat, A., et al. (2005). Climate change on the Yucatan

Peninsula during the little ice age. *Quat. Res.* 63 (2), 109–121. doi:10.1016/j.yqres.2004.11.004

Howard A. Johnson , D. H. Bredes, H. A., and Bredeson, D. H. (1971). Structural development of some shallow salt domes in Louisiana Miocene productive belt. *Bulletin* 55 (2), 204–226. doi:10.1306/5D25CE19-16C1-11D7-8645000102C1865D

Jones, C. E., and Blom, R. G. (2014). Bayou Corne, Louisiana, sinkhole: Precursory deformation measured by radar interferometry. *Geology* 42 (2), 111–114. doi:10.1130/G34972.1

J., T., and V., M. (2002). Karst geoindicators of environmental change: The case of Lithuania. *Environ. Geology.* 42 (7), 757–766. doi:10.1007/s00254-002-0553-8

Kiss, P. J., Tölgyesi, C., Bóni, I., Erdős, L., Vojtkó, A., Maák, I. E., et al. (2020). The effects of intensive logging on the capacity of karst dolines to provide potential microrefugia for cool-adapted plants. *Ags* 60 (1), 37–48. doi:10.3986/AGS.6817

Kovacs, S. E., van Hengstum, P. J., Reinhardt, E. G., Donnelly, J. P., and Albury, N. A. (2013). Late Holocene sedimentation and hydrologic development in a shallow coastal sinkhole on Great Abaco Island, the Bahamas. *Quat. Int.* 317, 118–132. doi:10.1016/j.quaint.2013.09.032

Linares, R., Roqué, C., Gutiérrez, F., Zarroca, M., Carbonel, D., Bach, J., et al. (2017). The impact of droughts and climate change on sinkhole occurrence. A case study from the evaporite karst of the Fluvia Valley, NE Spain. *Sci. Total Environ.* 579, 345–358. doi:10.1016/j.scitotenv.2016.11.091

Liu, R., Zhang, Z., Shen, J., and Wang, Z. (2019). Bryophyte diversity in karst sinkholes affected by different degrees of human disturbance. *Acta Soc. Bot. Pol.* 88 (2), 3620. doi:10.5586/asbp.3620

Louisiana Department of Natural Resources (2012). *Bayou Corne incident 2012*. Baton Rouge, LA: Louisiana Department of Natural Resources. Available at: http://dnr.louisiana.gov/index.cfm?md=pagebuilder&tmp=home&pid=939 (Last accessed October 11, 2021).

Montes-Ortiz, L., and Elias-Gutierrez, M. (2018). Faunistic survey of the zooplankton community in an oligotrophic sinkhole, Cenote Azul (Quintana Roo, Mexico), using different sampling methods, and documented with DNA barcodes. *J. Limnol* 77 (3), 428–440. doi:10.4081/jlimnol.2018.1746

Mostafiz, R. B., Friedland, C. J., Rohli, R. V., Gall, M., Bushra, N., and Gilliland, J. M. (2020a). Census-Block-Level Property Risk Estimation Due to Extreme Cold Temperature, Hail, Lightning, and Tornadoes in Louisiana, United States. *Front. Earth Sci.* 8, 601624. doi:10.3389/feart.2020.601624

Mostafiz, R. B., Friedland, C. J., Rohli, R. V., and Bushra, N. (2020b). "Assessing Property Loss in Louisiana, U.S.A., to Natural Hazards Incorporating Future Projected Conditions," in American Geophysical Union Conference, NH015–002. Available at: https://ui.adsabs.harvard.edu/abs/2020AGUFMNH0150002M/abstract (Accessed August 27, 2021).

Mostafiz, R. B., Friedland, C. J., Rohli, R. V., Bushra, N., and Held, C. L. (2021a). Property Risk Assessment for Expansive Soils in Louisiana. *Front. Built Environ.* 7, 754761. doi:10.3389/fbuil.2021.754761

Mostafiz, R. B., Friedland, C. J., Rohli, R. V., and Bushra, N. (2021b). "Census-block-level property risk assessment for wildfire in Louisiana, U.S.A.," in *review at Frontiers in Forests and Global Change since 7/13/2021*. Lausanne, Switzerland: Frontiers Media. Available at: https://www.essoar.org/doi/10.1002/essoar.10508248.2 (Last accessed October 13, 2011).

Mostafiz, R. B., Friedland, C. J., Rahman, M. A., Rohli, R. V., Tate, E., Bushra, N., et al. (2021c). Comparison of neighborhood-scale, residential property flood-loss assessment methodologies. *Front. Environ. Sci.* 9, 734294. doi:10.3389/fenvs.2021.734294

Mostafiz, R. B., Bushra, N., Rohli, R. V., Friedland, C. J., and Rahim , M. A. (2021d). Present vs. Future Property Losses from a 100-year Coastal Flood: A Case Study of Grand Isle, Louisiana. *Front. Water* 3, 763358. doi:10.3389/frwa.2021.763358

Nof, R. N., Baer, G., Ziv, A., Raz, E., Atzori, S., Salvi, S., et al. (2013). Sinkhole precursors along the Dead Sea, Israel, revealed by SAR interferometry. *Geology* 41 (9), 1019–1022. doi:10.1130/G34505.1

Orhan, O., Yakar, M., and Ekercin, S. (2020). An application on sinkhole susceptibility mapping by integrating remote sensing and geographic information systems. *Arabian J. Geosciences* 13 (17), 1–17. doi:10.1007/s12517-020-05841-6

Paine, J. G., Buckley, S. M., Collins, E. W., and Wilson, C. R. (2012). Assessing Collapse Risk in Evaporite Sinkhole-prone Areas Using Microgravimetry and Radar Interferometry. *Jeeg* 17, 75–87. doi:10.2113/JEEG17.2.75

Panno, S. V., Curry, B. B., Wang, H., Hackley, K. C., Zhang, Z., and Lundstrom, C. C. (2012). The effects of climate change on speleogenesis and karstification since the penultimate glaciation in southwestern Illinois' sinkhole plain. *Carbonates Evaporites* 27 (1), 87–94. doi:10.1007/s13146-012-0086-5

Peros, M., Collins, S., G'Meiner, A. A., Reinhardt, E., and Pupo, F. M. (2017). Multistage 8.2 kyr event revealed through high-resolution XRF core scanning of Cuban sinkhole sediments. *Geophys. Res. Lett.* 44 (14), 7374–7381. doi:10.1002/2017GL074369

Reynolds, S. J., Rohli, R. V., Johnson, J. K., Waylen, P. R., and Francek, M. A. (2021). *Exploring Physical Geography*. Third edition. McGraw-Hill: McGraw-Hill US Higher Ed USE.

Rucker, M. L., Panda, B. B., Meyers, R. A., and Lommler, J. C. (2013). Using InSAR to detect subsidence at brine wells, sinkhole sites, and mines. *Carbonates Evaporites* 28, 141–147. doi:10.1007/s13146-013-0134-9

Sharrar, A. M., Flood, B. E., Bailey, J. V., Jones, D. S., Biddanda, B. A., Ruberg, S. A., et al. (2017). Novel large sulfur bacteria in the metagenomes of groundwater-fed chemosynthetic microbial mats in the Lake Huron basin. *Front. Microbiol.* 8, 791. doi:10.3389/fmicb.2017.00791

Shunk, A. J., Driese, S. G., Farlow, J. O., Zavada, M. S., and Zobaa, M. K. (2009). Late Neogene paleoclimate and paleoenvironment reconstructions from the Pipe Creek Sinkhole, Indiana, USA. *Palaeogeogr. Palaeoclimatol. Palaeoecol.* 274 (3–4), 173–184. doi:10.1016/j.palaeo.2009.01.008

Swann, C. T. (1989). Review of geology of Mississippi salt domes involved in nuclear research. *Trans. – Gulf Coast Assoc. Geol. Societies* 39, 543–551. doi:10.1306/a1addc67-0dfe-11d7-8641000102c1865d

Szűcs, E., Gönczy, S., Bozsó, I., Bányai, L., Szakacs, A., Szárnya, C., et al. (2021). Evolution of surface deformation related to salt-extraction-caused sinkholes in Solotvyno (Ukraine) revealed by Sentinel-1 radar interferometry. *Nat. Hazards Earth Syst. Sci.* 21 (3), 977–993. doi:10.5194/nhess-21-977-2021

United States Army Corps of Engineers (2019). NSI Technical Documentation. Available at: https://www.hec.usace.army.mil/confluence/nsidocs/nsi-technical-documentation-50495938.html (Last accessed October 11, 2021).

United States Census Bureau (2020). Available at: https://www2.census.gov/programs-surveys/popest/datasets/ (Last accessed October 11, 2021).

United States Census Bureau (2010). TIGER/Line Shapefiles. Available at: https://www.census.gov/geographies/mapping-files/time-series/geo/tiger-line-file.2010.html (Last accessed October 11, 2021).

van Hengstum, P. J., Scott, D. B., Gröcke, D. R., and Charette, M. A. (2011). Sea level controls sedimentation and environments in coastal caves and sinkholes. *Mar. Geology.* 286 (1–4), 35–50. doi:10.1016/j.margeo.2011.05.004

Whyatt, J., and Varley, F. (2008). "Catastrophic failures of underground evaporite mines," in *Proceedings of the 27th International Conference on Ground Control in Mining*. Editors S. S. Peng, C. Mark, and G. Finfinger (Morgantown: West Virginia). , 29–31. Available at: https://www.cdc.gov/niosh/mining/UserFiles/works/pdfs/cfoue.pdf (Last accessed October 11, 2021).

Wu, Y., Tan, L., Liu, W., Wang, B., Wang, J., Cai, Y., et al. (2015). Profiling bacterial diversity in a limestone cave of the western Loess Plateau of China. *Front. Microbiol.* 6, 244. doi:10.3389/fmicb.2015.00244

Xiao, H., and Li, H. (2020). Modeling downward groundwater leakage rate to evaluate the relative probability of sinkhole development at an under-construction expressway and its vicinity. *Front. Earth Sci.* 8, 225. doi:10.3389/feart.2020.00225

Yang, G., Peng, C., Liu, Y., and Dong, F. (2019). Tiankeng: An ideal place for climate warming research on forest ecosystems. *Environ. Earth Sci.* 78 (2), 46. doi:10.1007/s12665-018-8033-y

Conflict of Interest: The authors declare that the research was conducted in the absence of any commercial or financial relationships that could be construed as a potential conflict of interest.

Publisher's Note: All claims expressed in this article are solely those of the authors and do not necessarily represent those of their affiliated organizations, or those of the publisher, the editors and the reviewers. Any product that may be evaluated in this article, or claim that may be made by its manufacturer, is not guaranteed or endorsed by the publisher.